Biochemical and Biophysical Research Communications 454 (2014) 151–156

Contents lists available at ScienceDirect

Biochemical and Biophysical Research Communications

journal homepage: www.elsevier.com/locate/ybbrc

Characterization of a T-superfamily conotoxin TxVC from *Conus textile* that selectively targets neuronal nAChR subtypes

Shuo Wang [a,1], Tianpeng Du [b,1], Zhuguo Liu [a], Sheng Wang [c], Ying Wu [c], Jiuping Ding [c], Ling Jiang [b,*], Qiuyun Dai [a,*]

[a] Beijing Institute of Biotechnology, Beijing 10071, China
[b] Key Laboratory of Magnetic Resonance in Biological Systems, National Center for Magnetic Resonance in Wuhan, State Key Laboratory of Magnetic Resonance and Atomic and Molecular Physics, Wuhan Institute of Physics and Mathematics, Chinese Academy of Science, Wuhan 430071, China
[c] Key Laboratory of Molecular Biophysics of the Ministry of Education, College of Life Science and Technology, Huazhong University of Science and Technology, Wuhan 430074, China

ARTICLE INFO

Article history:
Received 2 October 2014
Available online 18 October 2014

Keywords:
Conus textile
T-superfamily conotoxin TxVC
Neuronal nicotinic acetylcholine receptor
Selectivity
NMR structure

ABSTRACT

T-superfamily conotoxins have a typical cysteine pattern of "CC–CC", and are known to mainly target calcium or sodium ion channels. Recently, we screened the targets of a series of T-superfamily conotoxins and found that a new T-superfamily conotoxin TxVC (KPCCSIHDNSCCGL-NH_2) from the venom of *Conus textile*. It selectively targeted the neuronal nicotinic acetylcholine receptor (nAChR) subtypes α4β2 and α3β2, with IC_{50} values of 343.4 and 1047.2 nM, respectively, but did not exhibit obvious pharmacological effects on voltage-gated potassium, sodium or calcium channel in DRG cells, the BK channels expressed in HEK293 cells, or the Kv channels in LβT2 cells. The changes in the inhibitory activities of its Ala mutants, the NMR structure, and molecular simulation results based on other conotoxins targeting nAChR α4β2, all demonstrated that the residues Ile^6 and Leu^{14} were the main hydrophobic pharmacophores. To our best knowledge, this is the first T-superfamily conotoxin that inhibits neuronal nAChRs and possesses high binding affinity to α4β2. This finding will expand the knowledge of the targets of T-superfamily conotoxins and the motif information could help the design of new nAChR inhibitors.

1. Introduction

Conotoxins are secreted by Cone snails to subdue preys and defend against predators. A large number of conotoxin genes and proteins have been identified and categorized into various superfamilies (A, B, C, D, E, I, M, O, P, S, T, et al.), according to the number of cysteine residues, the arrangement of the disulfide bonds and the consensus signal sequences [1]. These conotoxins specifically target various ion channels such as Na^+, K^+, and Ca^{2+} channels and membrane receptors such as nAChR, 5-HT3R, NMDAR and G-protein-coupled receptors [2]. Some conotoxins are neuropharmacological reagents, and several have entered clinical trials. One conotoxin was even approved by FDA for pain treatment [3].

T-superfamily conotoxins typically contain CC–CC– cysteine pattern with a disulfide bond connectivity of I–III, II–IV, or CC–C–C pattern with a disulfide bond connectivity of I–IV, II–III. They selectively interact with Na^+ channels, presynaptic Ca^{2+} channels or G protein-coupled presynaptic receptors in general [4,5]. However, we isolated a T-superfamily conotoxin TxVC (KPCCSIHDNSCCGL-NH_2) from *C. textile* years ago, determined its peptide sequence by Edman method [6], investigated its disulfide bond configuration using the synthesized peptide, and then surprisingly found that this TxVC selectively interacted with neuronal nicotinic acetylcholine receptor (nAChR) subtype α4β2 and α3β2 without obvious pharmacological effects on voltage-gated K^+, Na^+ and Ca^{2+} ion channels in DRG cells. In order to probe its functional residues, its Ala mutants were generated and the inhibitory activities of those mutants were studied. The NMR structure of TxVC and molecular simulations based on other conotoxins targeting nAChR α4β2 revealed the key functional residues. To our best knowledge, this was the first T-superfamily conotoxin that was found to inhibit neuronal nAChRs particularly with high binding affinity to the α4β2 subtype. Our findings therefore expanded the knowledge of the T-superfamily conotoxin targets and this novel motif could be used to design new nAChR inhibitors.

2. Material and methods

2.1. Peptide synthesis

TxVC and its mutants were synthesized using the method described previously [7]. Briefly, the peptide was synthesized and

* Corresponding authors. Fax: +86 10 63833521.
E-mail addresses: lingjiang@wipm.ac.cn (L. Jiang), qy_dai@yahoo.com (Q. Dai).
[1] Shuo Wang and Tianpeng Du contributed equally to this work.

http://dx.doi.org/10.1016/j.bbrc.2014.10.055
0006-291X/

then cleaved from Rink resin with the cleavage solution [trifluoroacetic acid (TFA), 8.8 ml/water, 0.5 ml/DTT, 0.5 g/Triisopropylsilane, 0.2 ml]. The released peptides were oxidized in 0.1 M NH_4HCO_3 at room temperature, pH 8.0–8.2. The folded products were then purified using semi-preparative RP-HPLC. The final products were assessed using analytical reversed-phase HPLC. The primary sequences of TxVC and its analogue were listed in Table 1.

2.2. Disulfide bond analysis

Limited amount of the natural TxVC, which was formed during the one-step oxidative folding, only allowed its disulfide bond arrangement to be determined by comparison with the folded peptide products with known disulfide bond connectivity. The linear peptides containing acetamidomethyl (Acm) protected groups at positions C^2–C^4, C^1–C^4, or C^3–C^4 were folded in 0.1 M NH_4HCO_3 buffer (pH = 8.0) at room temperature for 24–48 h. The folded products were further oxidized with an iodine buffer containing 30% CH_3CN, 2% TFA, and 68% H_2O for 10 min to form different types of disulfide bond such as "C^1–C^3, C^2–C^4", "C^1–C^2, C^3–C^4", and "C^1–C^4, C^2–C^3". These secondary oxidized products were mixed with the one-step folding product of TxVC, and the disulfide bond connectivities were determined.

2.3. NMR spectroscopy

TxVC was dissolved in 500 μl 20 mM phosphate buffer (pH 5.5) containing 10% D_2O. NMR experiments, including TOCSY, NOESY and DQF-COSY, were conducted on a Bruker Avance 800 MHz spectrometer using TXI cryoprobe. All spectra were acquired at 303 K. The mixing times of TOCSY were 30 and 70 ms. The mixing times used for NOESY experiments were 300, 500, and 800 ms. H/D exchange experiment was performed at 303 K with addition of 500 μl D_2O to the lyophilized sample.

Spectra were processed using NMRPipe software and peak analyses were conducted with XEASY module in Cara (version 1.5.5) [8]. Spin systems were established based on DQF-COSY and TOCSY spectra. The NOE intensities of NOESY spectra with a 500 ms mixing time were extracted using CARA 1.8.4.2 and converted into distance constraints. $^3J_{H\alpha\text{-}NH}$ coupling constants were determined by DQF-COSY. A set of 100 structures was calculated using CYANA (version 2.1) with 171 nonredundant NOE constraints and 12 dihedral angle constraints. The final 20 conformers with the lowest energies were refined using Amber11. Disulfide bonds were identified by first measuring the internuclear distances in structures without disulfide bond constraints and then adding them into the final calculations. Seventy point eight percent of the phi-psi torsion angles in the structure were in the most favored regions in the Ramachandran plot according to Procheck. The three-dimensional structures were displayed using MOLMOL graphics program.

2.4. Inhibitory activity on nAChR subunits expressed in Oocyte

cRNA preparation, oocyte harvesting, and nAChR subunits expression were performed as previously described with modifications [9]. Each Xenopus oocyte was injected with at least 20 ng of cRNA and incubated with ND96 solution (96.0 mM NaCl, 2.0 mM KCl, 1.8 mM $CaCl_2$, 1.0 mM $MgCl_2$, and 5 mM HEPES, pH ~ 7.3) containing 2.5 mM pyruvic acid sodium (Sigma, St. Louis, MO) and antibiotics (100 U/mL penicillin, 100 mg/mL streptomycin, Sigma) at 18 °C. Data were recorded at day2 through day5 post-injection at room temperature (~22 °C).

The oocytes were gravity-perfused in a recording chamber (~50 μl) with ND96 at a rate of ~1.5 ml/min. The membrane potential was clamped at −70 mV and the ACh-gated currents were recorded with a two-electrode voltage-clamp amplifier (Axoclamp 900A, Axon Instruments Inc., USA). The current signals were digitized at 20 Hz with Axon Digidata 1440A (Axon Instruments Inc., USA) and low-pass filtered at 5 Hz. To measure the baseline responses, the oocytes were continuously perfused with ND96, during which ACh was automatically applied at 5 min intervals until peak current amplitude was obtained (3 s). To measure the dose response, the oocytes were continuously perfused with toxin solution until equilibrium (5–10 min) prior to the ACh pulse. AChs were prepared with ND96 at concentrations of 200 μM for α7, 30 μM for α9α10, and 100 μM for the others. TxVC solution contained 0.1 mg/ml BSA to reduce non-specific adsorption. In experiments with high doses (1 μM or greater), 5.5 μl of a 10-fold-concentrated toxin solution was added directly into the static bath for 5 min prior to ACh pulse exposure.

The dose-response data were fit to the equation: % response = $100/[1 + ([\text{toxin}]/IC_{50})^n]$, where n is the Hill coefficient and IC_{50} is the antagonist concentration giving half-maximal response, by non-linear regression analysis using GraphPad Prism (GraphPad Software, San Diego, CA).

2.5. Analyses of key residues of TxVC binding to nAChR α4β2

To date, only GIC (PDB ID 1UL2) and GID (PDB ID 1MTQ) have been reported as the potent inhibitors of nAChR α4β2 among the known conotoxins (Table 1) [17,18]. Therefore, their functional residues were compared with those from TxVC [10]. All the three α-conotoxins and their mutants were subject to standard molecular dynamics to obtain their stable conformations. First of all, the

Table 1
Sequences of TxVC, its mutant and other conotoxins that target nAChR α4β2.

Peptide	Sequence	IC_{50}	Refs.
TxVC	KP**CC**SIHDNS**CC**GL*	343 nM	This work
TxVC[K1A]	***A***P**CC**SIHDNS**CC**GL*	>10 μM	This work
TxVC[P2A]	***KA*****CC**SIHDNS**CC**GL*	>10 μM	This work
TxVC[I6A]	KP**CC**S***A***HDNS**CC**GL*	>10 μM	This work
TxVC[H7A]	KP**CC**SI***A***DNS**CC**GL*	>10 μM	This work
TxVC[L14A]	KP**CC**SIHDNS**CC**G***A****	>10 μM	This work
EI	RO**CC**YHPT**C**NMSNPQ**IC***	~50% inhibition at 10 μM peptide	[14]
SrIA	RT**CC**SROT**C**RMγYPγLCG*	~50% inhibition at 10 μM peptide	[14]
SrIB	RT**CC**SROT**C**RMEYPγLCG*	~50% inhibition at 10 μM peptide	[14]
AnIB	GG**CC**SHPA**C**AANNQDY**C***	~50% inhibition at 1 μM peptide	[15]
GIC	**GCC**SHPA**C**AGNNQH**IC***	309 nM	[16]
GID	IRGγ**CC**SNPA**C**RVNNOHV**C**^	152 nM	[17]
MII	**GCC**SNPV**C**HLEHSNL**C***	~500 nM	[9]

O: 4-trans-hydroxyproline; γ: γ-carboxyglutamate; ^: C-terminal carboxylate; *: C-terminal carboxamide. The conserved Cys residues are highlighted in bold.

missing atoms, including polar and nonpolar hydrogen atoms, were added. Those peptides were then solvated into different water box with different sizes according to their own sizes. These systems were next relaxed for 12 ns under the microcanonical (NPT) ensembles with a time step of 1 fs using the current version of DESMOND (2014.2). The equilibrated conformations were extracted for further analysis. Finally, all the refined conotoxin conformations were aligned to the reference conformation in PyMol Suite (The PyMOL Molecular Graphics System, Version 1.5.0.4, Schrodinger, LLC).

3. Results

3.1. Chemical identity of the synthesized TxVC and its analogues

Native TxVC was isolated from the crude venom of *C. textile* by RP-HPLC [6]. Synthesized TxVC and its analogues were assessed using analytical reversed-phase HPLC, and the results showed that their purities were all above 98%. The purified TxVC and the native TxVC had the same retention time as shown in Fig. 1A. All the peptides had the same expected molecular weights, which were determined using Ultraflex III TOF/TOF mass spectrometry (Bruker).

3.2. Disulfide bridge pattern of TxVC was I–III, II–IV

HPLC results of the one-step and two-step folding of the three different Acm protected linearized peptides were shown in Fig. 1B–D. The retention time of the native TxVC was identical to that of TxVC with a disulfide connectivity of I–III, II–IV formed in the two-step oxidation process; instead, the retention time of the native TxVC was different from that of the synthetic TxVC with a disulfide bond connectivity of I–IV, II–III or the synthetic TxVC with a disulfide bond connectivity of I–II, III–IV, indicating the native disulfide bond connectivity of TxVC was I–III, II–IV.

3.3. NMR structure of TxVC

The structural parameters of TxVC are shown in Table 2. The ensemble of the 20 lowest energy structures was shown in Fig. 2A, and the ribbon representation was shown in Fig. 2B. The peptide contains a hairpin-like loop from Cys^4 to Asn^9, stabilized by two hydrogen bonds between Ser^5 NH and Asp^8 O, and Ser^5 O and Asp^8 NH. The side chains of the residues inside this compact loop were well defined. The C terminus of TxVC that formed a helical structure, was in close contact with the N terminus. The terminal contacts were stabilized by two disulfide bonds, Cys^3–Cys^{11} and Cys^4–Cys^{12}, as illustrated by side chain lines in Fig. 2A.

3.4. TxVC selectively targeted nAChR α4β2 and α3β2 subtypes

TxVC mainly bound to nAChRs α4β2 and α3β2 with the IC_{50}s of 343.4 (283.3–416.4) nM and 1047.2 (748.0–1446.0) nM, respectively (Fig. 3A and B). It also exhibited weak binding activities to other nAChR subtypes such as α2β2, α2β4, α4β2, α4β4, α7, and

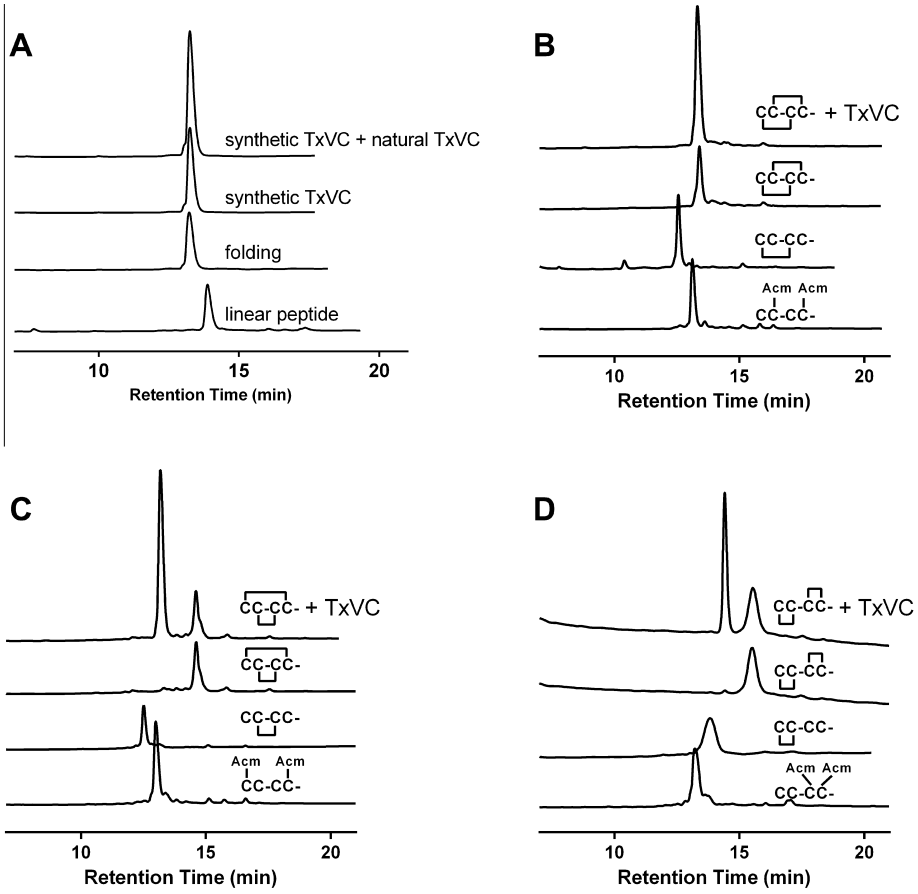

Fig. 1. HPLC analyses of the folded products of linear TxVC and its Acm derivatives. (A) One-step oxidative folding of TxVC. Traces from bottom to top: (a) linear peptide; (b) one-step oxidized products; (c) purified product; (d) co-elution of native TxVC and synthetic TxVC. (B) Determination of the disulfide bond connectivity of TxVC. Traces from bottom to top: (a) linear peptide with Acm modification at Cys2 and Cys4; (b) the first oxidized product; (c) the second oxidized product and (d) co-elution of the two-step folding products and one-step folding products. (C) and (D) determination of disulfide bond connectivity of TxVC with Acm modification at Cys1 and Cys4, Cys3 and Cys4, respectively. Samples were applied to a Calesil ODS-100 C18 column (4.6 mm × 250 mm) and eluted with a linear gradient of 0–1 min, 5–10% B; 1–25 min, 10–50% B; 25–28 min, 50–95% B, B is acetonitrile (0.1% TFA) at flow rate of 1 ml/min, 214 nm.

Table 2
Structural statistics of the ensemble of 20 structures of TxVC after CYANA calculation.

Parameter	Value
Target function	0.43
NOE distance constraints	171
Intra-residue	89
Sequential	45
Medium range ($1 < \|i-j\| < 5$)	16
Long range ($\|i-j\| \geq 5$)	21
Dihedral angle	12
NMR constraint violations	
Number of NOE violations ≧ 0.2 Å	0
Number of dihedral angle violations ≧ 5	0
RMSD deviation from the mean structure (Å)	
Backbone atoms	0.17 ± 0.06
Heavy atoms	0.59 ± 0.15
Ramachandran statistics obtained using PROCHECK-NMR	
Residues in most favored regions	70.0%
Residues in allowed regions	30.0%
Residues in disallowed regions	0

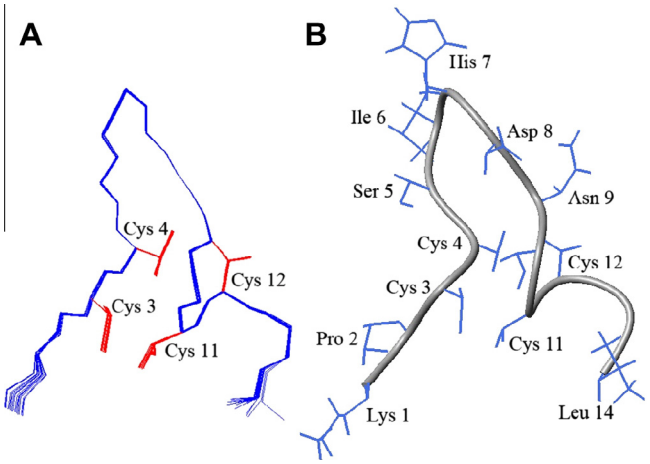

Fig. 2. NMR structure of TxVC. (A) Backbone ensemble of 20 lowest energy structures. The side chains of Cys residues are shown in red. (B) Ribbon representation of the closest-to-mean structure.

α9α10 with 50–60% inhibition at 10 μM concentration. When Lys[1], Pro[2], Ile[6], His[7] or Leu[14] was mutated to alanine, the binding ratio decreased to less than 50% at 10 μM concentration, suggesting the charges on the surface or at the hydrophobic pharmacophores of TxVC might be the main contributors to its binding activity.

4. Discussion

About 200 T-superfamily conotoxins have been deposited in the ConoServer database and a few are pharmacologically important [11]. T-superfamily conotoxins with a CC–CC cysteine pattern generally target voltage-sensitive Na^+ channel, presynaptic Ca^{2+} channel, or G protein-coupled presynaptic receptors. For example, ε-TxIX selectively reduces neurotransmitter release by reducing the presynaptic influx of Ca^{2+} [4,12], and Lt5d potently inhibits TTX-sensitive sodium currents in adult rat dorsal root ganglion neurons [13]. However, the present study showed that T-family conotoxin TxVC specifically inhibited neuronal nAChRs α3β2 and α4β2 Fig. 3), without significant effects on DRG Na^+, K^+ or Ca^{2+} channels (*see* Supplementary Fig. 1). TxVC did not act on the BK channels expressed in HEK293 cells or kV channels in LβT2 cells (data not shown), either, suggesting that it was unique. To our knowledge, TxVC is the first reported T-superfamily conotoxin that targets neuronal nAChRs. Currently, conotoxins from several families, including α-conotoxins, αS-conotoxins, and αC-conotoxins, have been found to inhibit nAChRs [2]. Among them, only a few α-conotoxins, such as GID, GIC, MII, AnIB, SrIA, SrIB and EI, target nAChR subtype α4β2 Table 1. SrIA, SrIB and EI presented weak inhibitory effects on α4β2 subtype (10 μM peptides inhibited nAChR α4β2 current by 50–60%) [14]. AnIB was slightly stronger, inhibiting nAChR α4β2 current by about 50% at 1 μM [15]. GID,

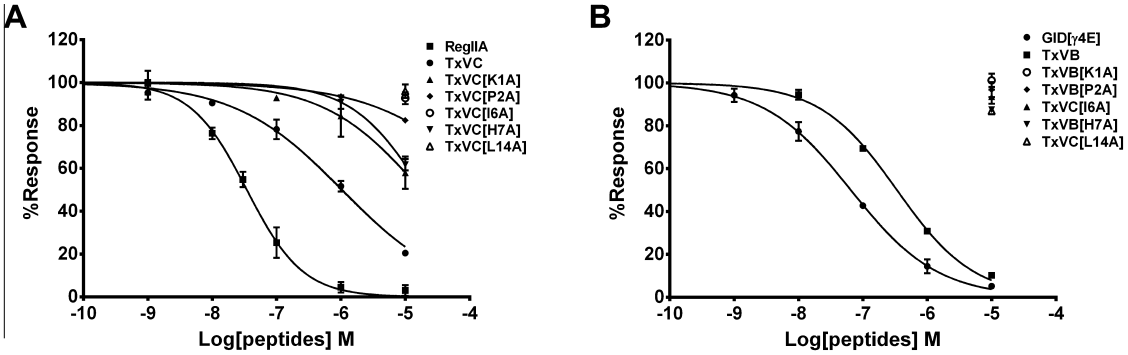

C

IC_{50} (nM)	α3β2	α4β2	α2β2	α2β4	α3β4	α4β4	α7	α9α10
RegIIA	34.5 (26.0 - 45.7)	-	-	-	-	-	-	-
GID[γ4E]	-	64.9 (52.6 - 80.2)	-	-	-	-	-	-
TxVC	1032.8 (758.9 – 1405.5)	343.4 (283.3 - 416.4)	>10000	>10000	>10000	>10000	>10000	>10000
TxVC[K1A]	>10000	>10000	>10000	>10000	>10000	>10000	>10000	>10000
TxVC[P2A]	>10000	>10000	>10000	>10000	>10000	>10000	>10000	>10000
TxVC[I6A]	>10000	>10000	>10000	>10000	>10000	>10000	>10000	>10000
TxVC[H7A]	>10000	>10000	>10000	>10000	>10000	>10000	>10000	>10000
TxVC[L14A]	>10000	>10000	>10000	>10000	>10000	>10000	>10000	>10000

Fig. 3. Effects of TxVC on rat nAChRs that were expressed in *Xenopus* Oocytes. (A) and (B) concentration–response curves of the rat α3β2 and α4β2 nAChR (n = 4–6). (C) IC_{50} of peptides on various rat nAChR subtypes. The control peptides of α3β2 and α4β2 were RegIIA (IC_{50} = 34.5 nM) and GID[γ4E] (IC_{50} = 64.9 nM), respectively. Peptides were applied by perfusion to oocytes expressing nAChRs as described in Section 2. "–", untested. Numbers in parentheses indicate 95% confidence intervals.

GIC and MII were very potent, inhibiting α4β2 subtype with IC_{50}s of 152 nM, 309 nM and 500 nM, respectively, and α3β2 subtype with even lower IC_{50}s, 3.1 nM, 1.1 nM and 0.5 nM, respectively. Therefore, their inhibitory effect ratios on α3β2 vs. α4β2 were ~50-fold, 300-fold and 1000-fold, respectively [9,16,17]. Therefore, TxVC was the third potent α4β2 inhibitor among all the natural conotoxins, and exhibited even higher selectivity on α4β2, with the α4β2 vs α3β2 selectivity ration of 3.

T-superfamily conotoxins with cysteine frame "CC–CC" could adopt three possible disulfide bond connectivities: globular (I–III, II–IV), ribbon (I–IV, II–III) and beads (I–II, III–IV), and the one in TxVC appeared to be the disulfide bond connectivity of I–III, I–IV. TxVC belongs to framework V of the T-superfamily conotoxins (Fig. 1), and to date only two conotoxins (ε-TxIX and τ-CnVA) from this superfamily have been characterized using NMR [18]. Interestingly, these two conotoxins share little common structure. The inter-cysteine loop number of TxVC and the residues involved are significantly different from those of ε-TxIX and τ-CnVA, and therefore their targets are different: ε-TxIX interacts with GPCR to reduce the Ca^{2+} presynaptic influx at a cholinergic synapse and τ-CnVA abolishes the agonist-induced activation of the sst3 receptor [4,19].

Since alpha-conotoxins GIC and GID target nAChR subtype α4β2 [20], their function residues were compared with those from TxVC. Molecular calculation showed that each of them had three functional residues adopting similar orientation to form specific pharmacophores. In GID, these residues are Ala^{10}, Val^{13} and Val^{18} with the first two residing only in the helix, whereas in GIC, they are Ala^{7}, Ala^{9} and Ile^{15} (Fig. 4). Consistently, the length of the aliphatic side-chain at position 13 in GID determined the receptor selectivity and the corresponding residue in GIC was at position 10 [17]. Although their N termini both had flexible conformations, the distance between these functional residues almost always stayed the same even after exhaustive molecular dynamics simulations (total simulation period was 12 ns with a time step of 1 fs). Structure alignment of TxVC with both GIC and GID revealed the overlap of Ile^{6} and Leu^{14} with those hydrophobic pharmacophores. However, the distance between Ile^{6} and Leu^{14} was slightly longer than those in GIC and GID. Additionally, TxVC lacked the helix, and therefore the conformations at both ends of the pharmacophore were more flexible and more hydrophobic. The replacement of Lys^{1}, Pro^{2}, Ile^{6}, His^{7} and Leu^{14} with Ala in TxVC also confirmed the hypothesis as the inhibitory activities of these mutants on α4β2 and α3β2 decreased significantly (Fig.3).

In addition to the typical cysteine framework CC–CC, other cysteine frameworks also exist in T-superfamily conotoxins, such as CC–C–C– and C–C–CC [21,22]. The targets of most of T-superfamily conotoxins with the above cysteine framework still remain unknown, except that a few were found to target alpha1-adrenoceptor or neuronal noradrenaline transporters [23].

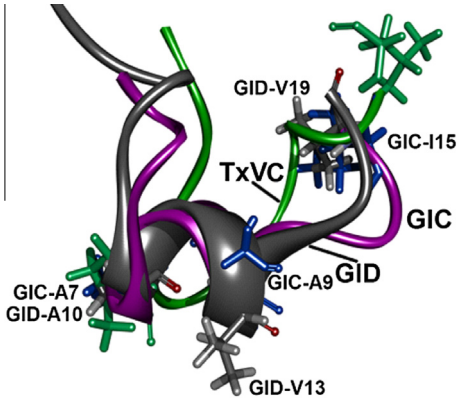

Fig. 4. Spatial orientation of the hydrophobic pharmacophores and key residues in GID (dark gray), GIC (purple) and TxVC (green) indicating their similar conformation. Key residues are indicated by sticks.

In conclusion, we found a new T-superfamily conotoxin TxVC targeting neuronal nAChR subtypes. This conotoxin was designated as αT-conotoxin, which expanded the knowledge of the existing T-superfamily conotoxins. The unique pharmacological sites of TxVC provided new insight into the biological activity of T-superfamily conotoxin, and the molecular structure could potentially be used for designing novel nAChRs probes.

Conflict of interest statement

The authors hereby declare that there are no conflicts of interest related to this study.

Acknowledgments

This work was supported by grants from the National Natural Sciences Foundation of China (No. 81173035) and the National Basic Research Program of China (No. 2010CB529802).

Appendix A. Supplementary data

Supplementary data associated with this article can be found, in the online version, at http://dx.doi.org/10.1016/j.bbrc.2014.10.055.

References

[1] S. Dutertre, A.H. Jin, Q. Kaas, A. Jones, P.F. Alewood, R.J. Lewis, Deep venomics reveals the mechanism for expanded peptide diversity in cone snail venom, Mol. Cell. Proteomics 12 (2013) 312–329.
[2] R.J. Lewis, S. Dutertre, I. Vetter, M.J. Christie, Conus venom peptide pharmacology, Pharmacol. Rev. 64 (2012) 259–298.
[3] M. Essack, V.B. Bajic, J.A. Archer, Conotoxins that confer therapeutic possibilities, Mar. Drugs 10 (2012) 1244–1265.
[4] A.C. Rigby, E. Lucas-Meunier, D.E. Kalume, E. Czerwiec, B. Hambe, I. Dahlqvist, P. Fossier, G. Baux, P. Roepstorff, J.D. Baleja, B.C. Furie, B. Furie, J. Stenflo, A conotoxin from *Conus textile* with unusual posttranslational modifications reduces presynaptic Ca^{2+} influx, Proc. Natl. Acad. Sci. U.S.A. 96 (1999) 5758–5763.
[5] C.A. Elliger, T.A. Richmond, Z.N. Lebaric, N.T. Pierce, J.V. Sweedler, W.F. Gilly, Diversity of conotoxin types from *Conus californicus* reflects a diversity of prey types and a novel evolutionary history, Toxicon 57 (2011) 311–322.
[6] C. Xiao, R. Bao, Y. Lin, Q. Dai, Isolation and characterization of the conotoxins of *Conus textile* from the South China Sea, Chin. J. Mar. Drugs 25 (2006) 22–27.
[7] Q. Dai, Z. Sheng, J.H. Geiger, F.J. Castellino, M. Prorok, Helix-helix interactions between homo- and heterodimeric gamma-carboxyglutamate-containing conantokin peptides and their derivatives, J. Biol. Chem. 282 (2007) 12641–12649.
[8] Z.Y. Chen, D.Y. Zeng, Y.T. Hu, Y.W. He, N. Pan, J.P. Ding, Z.J. Cao, M.L. Liu, W.X. Li, H. Yi, L. Jiang, Y.L. Wu, Structural and functional diversity of acidic scorpion potassium channel toxins, PLoS One 7 (2012) e35154.
[9] G.E. Cartier, D. Yoshikami, W.R. Gray, S. Luo, B.M. Olivera, J.M. McIntosh, A new alpha-conotoxin which targets alpha3beta2 nicotinic acetylcholine receptors, J. Biol. Chem. 271 (1996) 7522–7528.
[10] Kevin J. Bowers, Edmond Chow, Huafeng Xu, Ron O. Dror, Michael P. Eastwood, Brent A. Gregersen, John L. Klepeis, István Kolossváry, Mark A. Moraes, Federico D. Sacerdoti, John K. Salmon, Yibing Shan, and David E. Shaw, Scalable Algorithms for Molecular Dynamics Simulations on Commodity Clusters, in: Proceedings of the ACM/IEEE Conference on Supercomputing (SC06), Tampa, Florida, November 11–17, 2006.
[11] Q. Kaas, R. Yu, A.H. Jin, S. Dutertre, D.J. Craik, ConoServer: updated content, knowledge, and discovery tools in the conopeptide database, Nucleic Acids Res. 40 (2012) D325–330.
[12] K.A. Bush, J. Stenflo, D.A. Roth, E. Czerwiec, A. Harrist, G.S. Begley, B.C. Furie, B. Furie, Hydrophobic amino acids define the carboxylation recognition site in the precursor of the γ-carboxyglutamic-acid-containing conotoxin ε-TxIX from the marine cone snail *Conus textile*, Biochemistry 38 (1999) 14660–14666.
[13] J. Liu, Q. Wu, C. Pi, Y. Zhao, M. Zhou, L. Wang, S. Chen, A. Xu, Isolation and characterization of a T-superfamily conotoxin from *Conus litteratus* with targeting tetrodotoxin-sensitive sodium channels, Peptides 28 (2007) 2313–2319.
[14] E. Lopez-Vera, M.B. Aguilar, E. Schiavon, C. Marinzi, E. Ortiz, R. Restano Cassulini, C.V. Batista, L.D. Possani, E.P. Heimer de la Cotera, F. Peri, B. Becerril, E. Wanke, Novel alpha-conotoxins from *Conus spurius* and the alpha-conotoxin

EI share high-affinity potentiation and low-affinity inhibition of nicotinic acetylcholine receptors, FEBS J. 274 (2007) 3972–3985.
[15] M.L. Loughnan, A. Nicke, A. Jones, D.J. Adams, P.F. Alewood, R.J. Lewis, Chemical and functional identification and characterization of novel sulfated alpha-conotoxins from the cone snail *Conus anemone*, J. Med. Chem. 47 (2004) 1234–1241.
[16] J.M. McIntosh, C. Dowell, M. Watkins, J.E. Garrett, D. Yoshikami, B.M. Olivera, Alpha-conotoxin GIC from *Conus geographus*, a novel peptide antagonist of nicotinic acetylcholine receptors, J. Biol. Chem. 277 (2002) 33610–33615.
[17] A. Nicke, M.L. Loughnan, E.L. Millard, P.F. Alewood, D.J. Adams, N.L. Daly, D.J. Craik, R.J. Lewis, Isolation, structure, and activity of GID, a novel alpha 4/7-conotoxin with an extended N-terminal sequence, J. Biol. Chem. 278 (2003) 3137–3144.
[18] R. Zamora-Bustillos, M.B. Aguilar, A. Falcon, E.P. Heimer de la Cotera, Identification, by RT-PCR, of four novel T-1-superfamily conotoxins from the vermivorous snail *Conus spurius* from the Gulf of Mexico, Peptides 30 (2009) 1396–1404.
[19] C. Petrel, H.G. Hocking, M. Reynaud, G. Upert, P. Favreau, D. Biass, M. Paolini-Bertrand, S. Peigneur, J. Tytgat, N. Gilles, O. Hartley, R. Boelens, R. Stocklin, D. Servent, Identification, structural and pharmacological characterization of tau-CnVA, a conopeptide that selectively interacts with somatostatin sst3 receptor, Biochem. Pharmacol. 85 (2013) 1663–1671.
[20] C. Lee, S.H. Lee, D.H. Kim, K.H. Han, Molecular docking study on the alpha3beta2 neuronal nicotinic acetylcholine receptor complexed with alpha-conotoxin GIC, BMB Rep. 45 (2012) 275–280.
[21] R.A. Balaji, A. Ohtake, K. Sato, P. Gopalakrishnakone, R.M. Kini, K.T. Seow, et al., λ-Conotoxins, a new family of conotoxins with unique disulfide pattern and protein folding. Isolation and characterization from the venom of *Conus marmoreus*, J. Biol. Chem. 275 (2000) 39516–39522.
[22] J.M. McIntosh, G.O. Corpuz, R.T. Layer, J.E. Garrett, J.D. Wagstaff, G. Bulaj, A. Vyazovkina, D. Yoshikami, L.J. Cruz, B.M. Olivera, Isolation and characterization of a novel conus peptide with apparent antinociceptive activity, J. Biol. Chem. 275 (2000) 32391–32397.
[23] I.A. Sharpe, J. Gehrmann, M.L. Loughnan, L. Thomas, D.A. Adams, A. Atkins, E. Palant, D.J. Craik, D.J. Adams, P.F. Alewood, R.J. Lewis, Two new classes of conopeptides inhibit the alpha1-adrenoceptor and noradrenaline transporter, Nat. Neurosci. 4 (2001) 902–907.